Available online at www.sciencedirect.com
SCIENCE DIRECT®
Journal of Power Sources 128 (2004) 135–144
JOURNAL OF POWER SOURCES
www.elsevier.com/locate/jpowsour

Study of NiO cathode modified by ZnO additive for MCFC

Bo Huang [a,*], Fei Li [a], Qing-chun Yu [b], Gang Chen [a], Bin-yuan Zhao [a], Ke-ao Hu [a,b]

[a] *State Key Laboratory of Metal Matrix Composites, Shanghai Jiaotong University, Huashan Road 1954, Shanghai 200030, PR China*
[b] *Institute of Fuel Cell, Shanghai Jiaotong University, Shanghai 200030, PR China*

Received 18 June 2003; received in revised form 10 September 2003; accepted 15 October 2003

Abstract

The preparation and subsequent oxidation of nickel cathodes modified by impregnation with zinc oxide (ZnO) were evaluated by surface and bulk analysis. The electrochemical behaviors of ZnO impregnated NiO cathodes was also evaluated in a molten 62 mol% Li_2CO_3 + 38 mol% K_2CO_3 eutectic at 650 °C by electrochemical impedance spectroscopy (EIS) as a function of ZnO content and immersion time. The ZnO impregnated nickel cathodes showed the similar porosity, pore size distribution and morphology to the reference nickel cathode. The stability tests of ZnO impregnated NiO cathodes showed that the ZnO additive could dramatically reduce the solubility of NiO in a eutectic carbonate mixture under the standard cathode gas condition. The impedance spectra for cathode materials show important variations during the 100 h of immersion. The incorporation of lithium in its structure and the low dissolution of nickel oxide and zinc oxide are responsible of these changes. After that, the structure reaches a stable state. The cathode material having 2 mol% of ZnO showed a very low dissolution and a good catalytic efficiency close to the NiO value. We thought that 2 mol% ZnO/NiO materials would be able to adapt as alternative cathode materials for MCFCs.

Keywords: Molten Carbonate Fuel Cell; Cathode; Solubility; Nickel oxide; Zinc oxide; EIS

1. Introduction

The molten carbonate fuel cell (MCFC) is believed to be one of the most promising energy conversion devices that convert chemical energy in fossil fuels into electricity in the near future owing to the high energy conversion efficiency, the excellent environmental characteristics and the ability to utilize a wide variety of fuels such as hydrogen, natural gas and coal gasified gas. However, several hurdles remain before commercialization of MCFC can be realized. The state-of-the-art MCFC nickel cathode, oxidized in situ and lithiated ($Li_xNi_{1-x}O$), presents a relatively high solubility in the electrolyte which can be Li_2CO_3/K_2CO_3, Li_2CO_3/Na_2CO_3 or related alkali molten carbonate eutectics. This dissolution leads to the formation of Ni^{2+}, which can diffuse from the cathode toward the anode under a concentration gradient. The dissolved Ni^{2+} precipitates in the sections of matrix, where it encounters dissolved H_2 proceeding from the anode side and is reduced to Ni at a certain distance away from the cathode. The continuous diffusion of Ni^{2+} accelerates more dissolution of nickel from the cathode. Continued deposition of sufficient bridged grains of metallic nickel across the cell eventually causes a short-circuiting of the cell [1,2]. The NiO dissolution also results in loss of active material and a decrease of the active surface area available for the oxygen reduction reaction resulting in degradation of fuel cell performance and durability.

Many efforts have been made to solve the NiO dissolution problem [3–7] and several possible approaches have been studied. More basic molten carbonate melts such as Li/Na carbonate eutectic have been used to decrease the Ni dissolution rate in the melt. Alkaline earth metal salts based on Ba or Sr have also been used as additives to increase the basicity of the melt. However, using more basic molten carbonate melts only partially solves the problem, since these melts decrease the NiO dissolution rate by 10–15% only. In addition, several materials like $LiFeO_2$, $LiCoO_2$, Li_2MnO_3 and $La_{1-x}Sr_xCoO_3$ were also investigated as replacement materials for the NiO cathodes because of their extremely low solubility in the carbonate melts [8]. However, the exchange current density for the oxygen reduction reaction on $LiFeO_2$, Li_2MnO_3 and $La_{1-x}Sr_xCoO_3$ is about two to four orders of magnitude lower than that on NiO. Thus, the slow kinetics of the oxygen reduction reaction limits further improvement of cathodes based on these materials. $LiCoO_2$ is

* Corresponding author. Tel.: +86-21-62933751; fax: +86-21-62822012.
E-mail address: huangbo2k@hotmail.com (B. Huang).

0378-7753/$ – see front matter © 2003 Elsevier B.V. All rights reserved.
doi:10.1016/j.jpowsour.2003.10.008

more stable than NiO in alkaline environment and is once considered as the most promising alternative cathode material. However, application of $LiCoO_2$ as a cathode material is still limited for producing large area electrodes beyond 1000 cm^2 because of its brittleness and higher manufacturing cost and less electronic conductivity than the conventional NiO cathode. Therefore, these oxides might be inadequate for the cathode material. Recently, new candidate materials such as $LiCoO_2$($LiFeO_2$, $La_{0.8}Sr_{0.2}CoO_3$)-coated NiO have been proposed [9–11].

The most promising way to modify the properties of nickel oxide appeared to be the incorporation of metal oxides to the nickel oxide [12–15]. In this paper, a novel cathode material has been prepared based on modifying NiO by zinc oxide impregnation, in order to decrease cathode dissolution rate and increase its catalytic activity for oxygen reduction. The present paper is aimed to study the effect of ZnO content on the electrochemical behavior of the new cathode materials in molten carbonates. The study has been conducted using electrochemical impedance spectroscopy (EIS). The phases and microstructures of the cathode materials before and after immersion in molten carbonate were analyzed by X-ray diffraction (XRD) and scanning electron microscopy (SEM), respectively. The dissolution of the new cathode material in molten carbonates was evaluated using melt analysis.

2. Experimental

2.1. Starting materials

The material system used in this work was based on carbonyl nickel powder, zinc oxide powder, solvent, dispersant, binder and plasticizer. The carbonyl nickel particles (purity: 98%; Shanghai Jinjiang Metal Powder Ltd., China) have a perfect orbicular shape and a narrow size distribution of 2.2–2.8 μm. The ZnO powder was of an analytical grade (Shanghai Chen. Ltd., China). The solvent system used in this paper consisted of azeotropic mixture of cyclohexanone and butyl alcohol in order to avoid differential evaporation. Glycerol trioleate as a kind of zwitterionic dispersant was used as dispersant. Poly-vinyl-butyl (PVB) and polyethylene glycol (PEG 200) were used as binder and plasticizer, respectively. The PVB binder was supplied as a free flowing fine-grained powder and the PEG plasticizer was obtained in a liquid form. All the organic additives were supplied by Shanghai Chem. Ltd., China.

2.2. Tape casting

Porous ZnO/NiO cathodes were prepared by a tape casting and subsequent sintering process. The slurries for the tape casting process were fabricated by a ball milling method that included two steps [16]. In the first step, 50 g of nickel power containing 0, 2, 6, 10, and 20 mol% ZnO powder were added to 1 g dispersant. The ingredients were mixed thoroughly with 40 g cyclohexanone/butyl alcohol solvents and the slurry was ball milled for 4 h in order to break weak agglomerates. Secondly, 5 g PVB and 5 g PEG were added to the above system and the resulting slurry was ball milled for an additional 4 h. After the mixing and the homogenization of the slurry were completed, the slurry was degassed using a vacuum pump (pressure: 200 mbar absolute) and cast on a casting surface of polyethylene film by a “doctor-blade” method. The cast tapes were allowed to dry at room temperature for 48 h. After the solvent in the tapes was completely evaporated, the nickel green tapes were obtained.

2.3. Sintering

Sintering temperature of the tape cast cathodes influences the cathode pore structure and thereby affects its electrochemical performance. Thermo gravimetric analysis (TGA) was done to determine the optimum heat treatment schedule for sintering. A typical TGA curve for green 2 mol% ZnO/Ni tape is shown in Fig. 1. The cast 2 mol% ZnO/Ni tape was pre-heated at 150 °C for 12 h in order to remove all the solvent in the tape. TGA analysis was done by heating the sample from 100 to 650 °C at a rate of 10 °C/min. A steep reduction in weight (13.5%) was seen on heating the sample between 200 and 400 °C due to the removal of the binder and plasticizer. The removal of all volatile and decomposable organic matter was completed below 400 °C. Fig. 2 shows the SEM of 2 mol% ZnO/Ni material obtained by tape casting and sintering at 850 °C in 75 vol.% H_2/25 vol.% N_2 atmosphere and air. It is evident that tapes sintered at 850 °C all show a perfectly open pore structure. Based on the above TGA and SEM analysis, the following heating sequence was used for sintering the porous cathodes. (1) the green tapes were initially heated from room temperature to 200 °C at a rate of 1 °C/min; (2) in the second step, the temperature was held at 200 °C for 2 h; (3) thirdly, the temperature was raised to 400 °C at a rate of 1 °C/min; (4) the temperature was held at 400 °C for 4 h; (5) the temperature was raised to 500 °C at a rate of 2 °C/min; (6) the temperature was held at 500 °C for 2 h; (7) the temperature was raised to 850 °C at a rate of 2 °C/min; (8) the temperature was held at 850 °C for 6 h; (9) in the last step, the samples was cooled to room temperature at a cooling rate of 1 °C/min. Sintering of the green tapes was completed in 75 vol.% H_2/25 vol.% N_2 atmosphere and air, respectively.

2.4. Electrochemical characterization

The electrochemical characterization of the new cathode materials was performed on the porous electrode/molten carbonates interface by means of EIS. The test cell was an alumina crucible contained in a covered quartz vessel. The cover of vessel had been adapted to accommodate a thermocouple, a gas inlet/outlet and two electrodes. The working electrode was composed of the new cathode material connected to a Pt lead (0.5 mm in diameter) that is shielded from

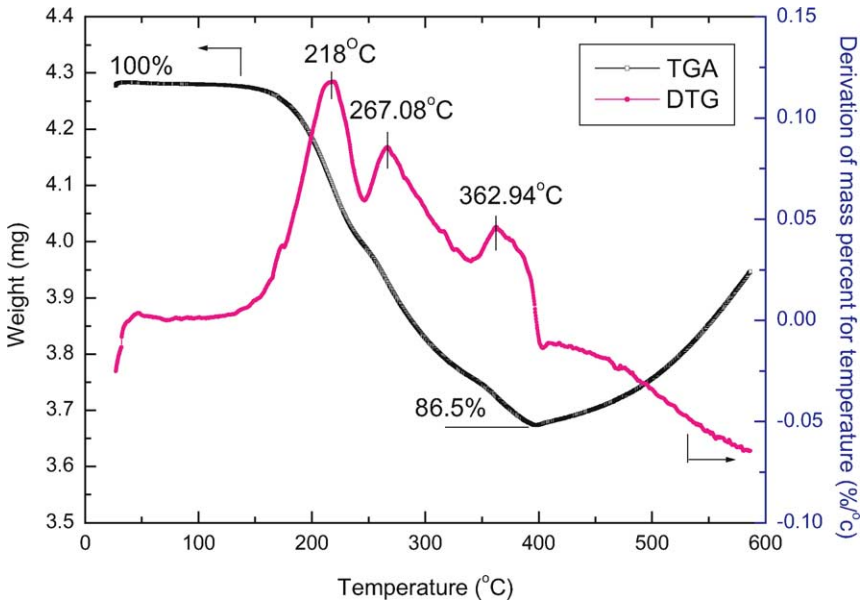

Fig. 1. The TGA/DTG curves of 2 mol% ZnO/Ni green tape obtained by non-aqueous tape casting.

the electrolyte by an alumina tube sealed by ceramic cement at the base of the tube. The counter electrode was identical to the working electrode. Such a configuration allows elimination of the influence of the counter electrode and avoids the use of a reference electrode that is, by itself, a source of noise [17,18]. Digital mass flow controllers/meters were used to provide the desired gas mixture composition of CO_2 and O_2. The gas mixture was flowed into the melt through a long alumina tube.

The crucible was charged with 300 g eutectic carbonate mixture (62 mol% Li_2CO_3–38 mol% K_2CO_3) and heated to 650 °C in a electric furnace. The eutectic mixture of alkali carbonate, 62 mol% Li_2CO_3–38 mol% K_2CO_3, was made up from AR grade anhydrous reagents (Shanghai Chem. Ltd., China) that had been dried in a furnace at 150 °C. The mixture was purified by a sequence of the following treatments: vacuum drying at 350 °C, fusion/pumping treatment at 700 °C and bubbling of pure CO_2 with the view of neutralizing any O^{2-} formed and decomposing any OH^- ion present. This purification procedure was basically similar to that proposed by Appleby and Nicholson [19]. Gases were of high purity grade and were additionally treated with molecular sieves 5 Å and anhydrous $Mg(ClO_4)_2$ to remove traces of water [20].

Then the electrodes (Φ : 2.4 cm × 0.08 mm) cut out from sintered NiO and ZnO/NiO plates in air were inserted in the carbonate melt and the cell temperature was kept at 650 °C. The EIS measurements were started 2 h after immersion in the melt in order to obtain a sufficiently stabilized system necessary for an ac-impedance experiment. Various measurements were made from 2 to 200 h under a 0.67 atm CO_2–0.33 atm O_2 gas mixture. The impedance spectra were recorded with a frequency response analyzer Solartron 1260. A 5 mV perturbation amplitude was applied with a frequency scanning range of 10 mHz–100 kHz at five points per frequency decade.

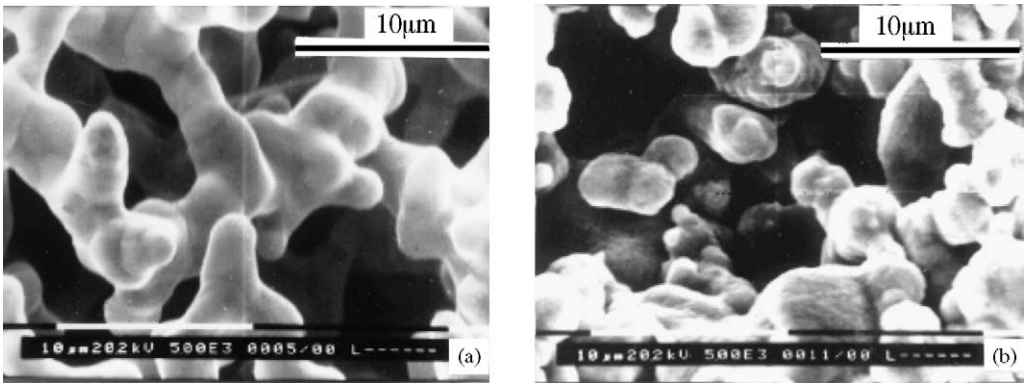

Fig. 2. SEM micrographs of (a) 2 mol% ZnO/Ni plate sintered at 850 °C in 75 vol.% H_2/25 vol.% N_2 atmosphere; (b) 2 mol% ZnO/Ni plate sintered at 850 °C in air.

2.5. Structural characterization and chemical analysis

The structure of the samples sintered at 850 °C for 6 h before and after the electrochemical tests was characterized by scanning electron microscopy (SEM, PHLIPS 515) and X-ray diffraction (XRD, D/max-3A, Cu Kα) at the scanning speed of 4°/min. In order to determine the structure of the samples after immersion in the molten carbonate, they should be first dissolved in 50 vol.% acetic acid/50 vol.% anhydride mixture aimed to removing the carbonates at the samples surface. Solubility was determined by removing a 0.5 g of molten carbonate from the melts at the appointed time using an alumina rod. Solubility measurements were repeated until their value became concentration that was regarded as the equilibrium solubility. Inductively coupled plasma spectroscopy was carried out to analyze the metal ions equilibrium solubility in the molten carbonate after 200 h of continuous exposure to the molten carbonate.

3. Results and discussion

3.1. Microstructural characterization

3.1.1. Cathode characterization

Table 1 shows textural characterization of the cathodes prepared. It can be seen that the oxidation processes produced a decrease of the porosity in both the nickel plate and ZnO/nickel plates. However, the porosities and pore size distributions of the modified NiO cathodes increased with the amount of ZnO additives, which was due to that the oxide additive hindered the sintering of the nickel particles during the heat-treatment process in a reducing atmosphere. Here, it should be noted that the nickel cathode with 20 mol% ZnO had so poor sintering performance that it had a low strength and was easily broken, which indicates that the additive amount should be limited.

3.1.2. SEM characterization

Fig. 3 shows the surface microstructures of pure nickel and various modified nickel cathodes. As shown in Fig. 3, all modified nickel cathodes had similar porous structures to the nickel cathode and a particle size slight higher than the nickel cathode. Fig. 4 shows the surface microstructures of pure nickel oxide and various modified nickel oxide cathodes after the electrochemical testing in the eutectic melt for 100 h. After the electrochemical testing, the cathode materials showed morphological changes due to the oxidation in air and dissolution in the molten carbonates of nickel and various modified nickel cathodes.

Table 1
Textural characterizations of prepared cathodes by mercury porosimetry

Cathode	Porosity (%)	Pore diameter (μm)
Ni	65.82	6.68
NiO	61.86	5.82
2 mol% ZnO/Ni plate	67.23	6.75
2 mol% ZnO/NiO plate	63.25	6.21
6 mol% ZnO/Ni plate	66.96	7.22
6 mol% ZnO/NiO plate	64.58	6.73
10 mol% ZnO/Ni plate	73.23	7.58
10 mol% ZnO/NiO plate	66.52	6.98
20 mol% ZnO/Ni plate	–	–
20 mol% ZnO/NiO plate	–	–

Table 2
Content of metal ions of ZnO/NiO cathode after immersion in Li/K eutectic melts for 200 h (atmosphere: 0.67 atm CO_2/0.33 atm O_2; T = 650 °C)

Sample	Content of ZnO	Ni^{2+} (mol ppm)	Zn^{2+} (mol ppm)
1	0 mol%	35.4	/
2	2 mol%	2.32	14.18
3	6 mol%	2.14	15.04
4	10 mol%	2.04	14.98
5	20 mol%	1.98	15.62

3.1.3. XRD characterization

Fig. 5 shows the X-ray diffraction (XRD) profiles of ZnO, NiO and ZnO/NiO cathodes. It can be seen from Fig. 5 that the peaks of the NiO cathode with 2 and 6 mol% ZnO additive are similar to that of pure NiO. However, when the amount of ZnO in NiO is over 10 mol%, some weak peaks that belong to ZnO can be detected.

Fig. 6 shows the XRD profiles of pure NiO and modified NiO cathodes that had been immersed in Li/K carbonate melts for 200 h. It can be seen that the XRD peaks of ZnO have been disappeared for the modified NiO cathodes with 10 and 20 mol% ZnO additive.

3.2. Solubility test

The solubility of various NiO cathodes after immersion in Li/K eutectic melts for 200 h is given in Table 2. The experimental conditions were kept at 650 °C under a 0.67 atm CO_2/0.33 atm O_2 atmosphere. The NiO cathode had a solubility of about 35 mol ppm (Ni^{2+}) after 200 h, which is similar to the results reported by Motohira et al. [13]. In contrast, the solubility of the NiO cathodes impregnated with 2 mol% ZnO was only 2.32 mol ppm (Ni^{2+}). With the increase of ZnO amount in NiO, the solubility of the modified cathodes decreased slightly. It can be seen that the ZnO additive has a strong positive effect on the reduction of NiO dissolution in carbonate melts. In addition, Table 2 also shows the concentration of Zn^{2+} dissolved in the carbonate melts as a function of the added ZnO content in the stabilized NiO cathode after 200 h. The concentration of Zn^{2+} in the carbonate melts increased with the increase of ZnO content in NiO cathodes. Here it should be noted that the concentration of Zn^{2+} was far more than that of Ni^{2+} in the carbonate melts.

It is well known that the NiO cathode is not stable during the MCFC operation. The material dissolves in the carbonate melts, resulting in the formation of Ni^{2+}, which can diffuse

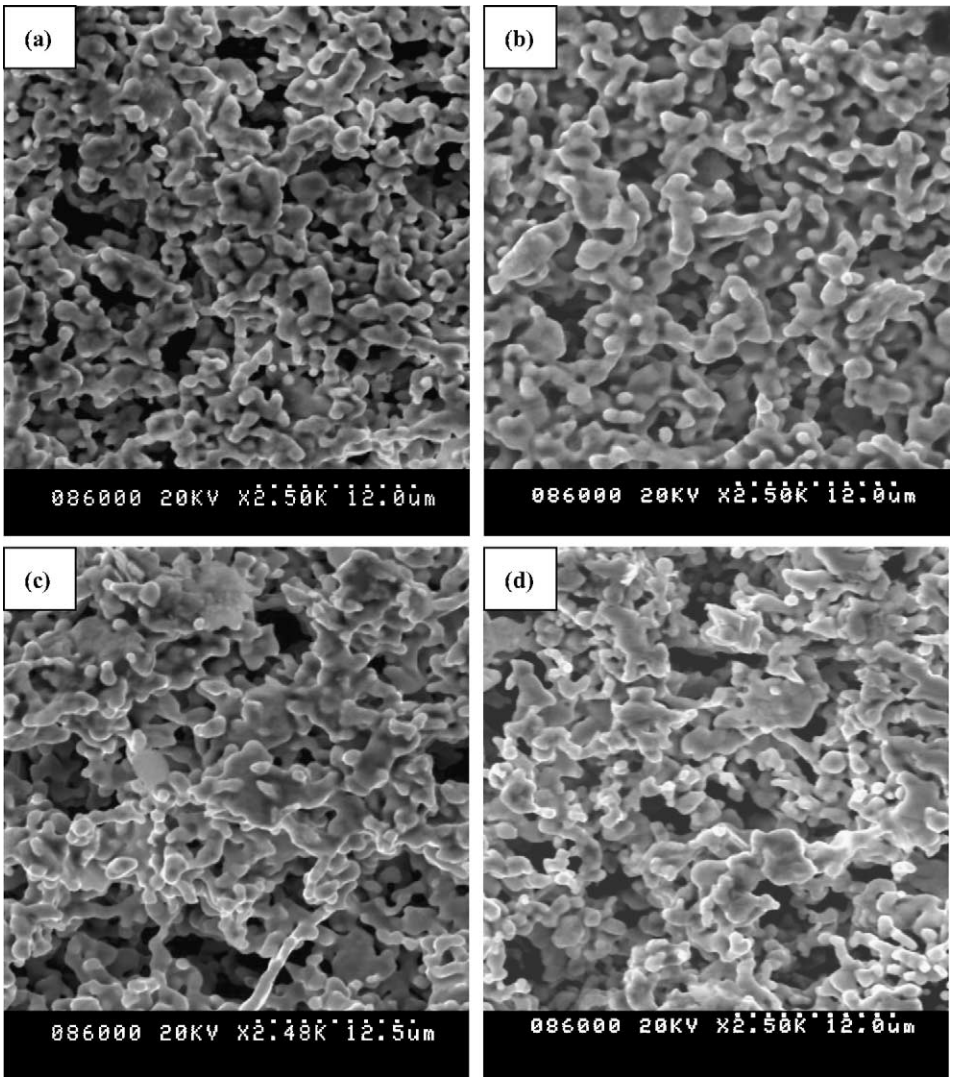

Fig. 3. SEM micrographs of ZnO/Ni cathode obtained in 75 vol.% H_2/25 vol.% N_2 atmosphere at 850 °C: (a) pure Ni (b) 2 mol% ZnO/Ni (c) 6 mol% ZnO/Ni (d) 10 mol% ZnO/Ni.

from the cathode toward the anode under a concentration gradient. The dissolved Ni^{2+} precipitates in the sections of matrix, where it encounters dissolved H_2 proceeding from the anode side and is eventually reduced to Ni at a certain distance away from the cathode. The dissolution reaction of NiO cathode and Ni metal precipitation can be written as the following equations:

$$NiO(s) \leftrightarrow Ni^{2+}(l) + O^{2-}(l) \quad (1)$$

$$Ni^{2+}(l) + H_2(g, l) \leftrightarrow Ni(s) + 2H^{+}(l) \quad (2)$$

On the other hand, the ZnO additive can also dissolve in the melts in the similar way, which is described as following equation:

$$ZnO(s) \leftrightarrow Zn^{2+}(l) + O^{2-}(l) \quad (3)$$

The solubility of ZnO in the carbonate melts was far more than that of NiO. Consequently, concentration of O^{2-} was increased in the micro region containing ZnO and NiO due to the preferential dissolution of ZnO. That was to say, increase of concentration of O^{2-} was inadvantageous for the formation of Ni^{2+} ion from the standpoint of view of dissolution equilibrium of NiO. In addition, according to Fig. 6, we could find that the diffraction peak of ZnO was completely vanished after immersion in Li/K carbonate melts for 200 h at 650 °C. Evidently, the dissolution of NiO was depressed due to the preferential dissolution of ZnO.

3.3. Electrochemical impedance spectroscopy (EIS) study

Fig. 7 depicts the electrochemical impedance spectra for the three cathode materials in a eutectic 62 mol% Li_2CO_3 + 38 mol% K_2CO_3 at 650 °C under a 0.67 atm CO_2/0.33 atm O_2 gas mixture at different immersion time. As it can be seen from the corresponding Nyquist plots, the impedance response of the three samples at different immersion time is characterized by the presence of high frequency loop and

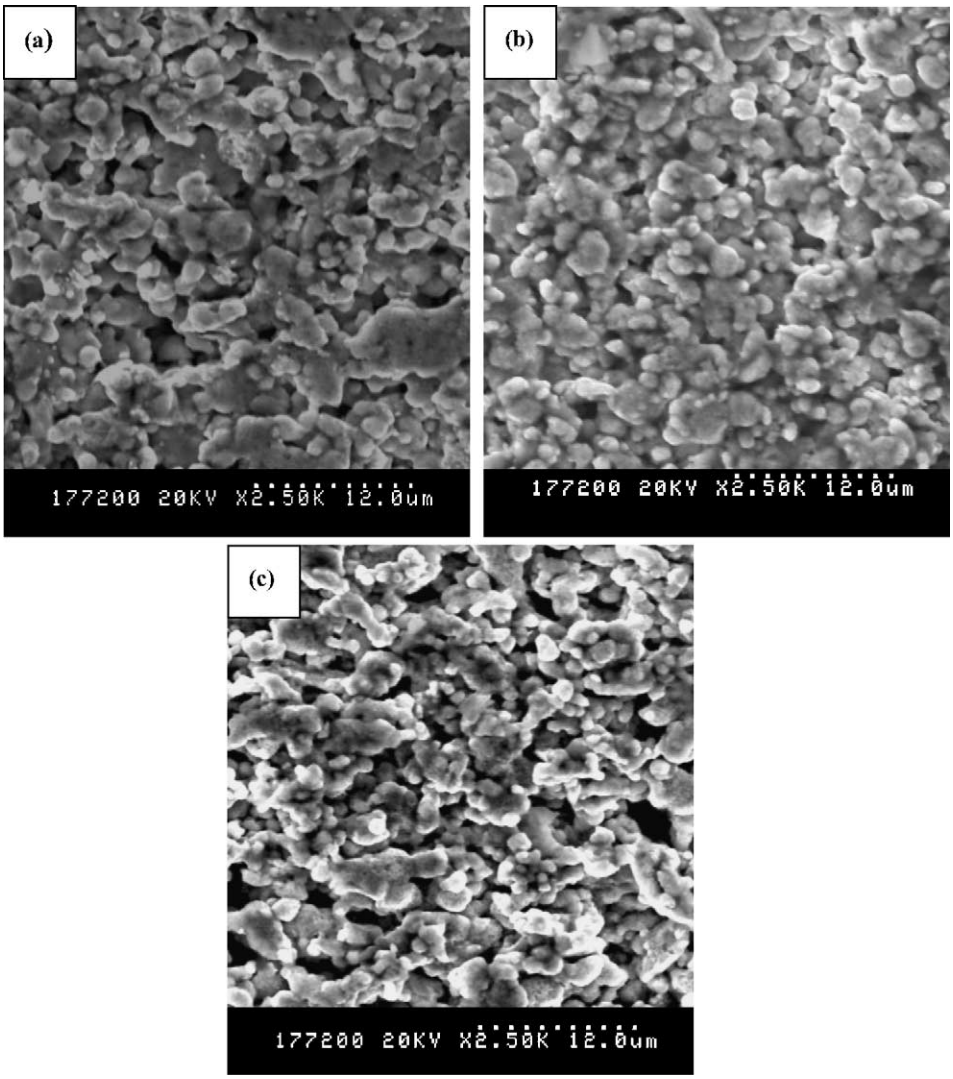

Fig. 4. SEM micrographs for the samples after testing (a) NiO; (b) 2 mol% ZnO/NiO; (c) 6 mol% ZnO/NiO.

an extension at low frequency, indicating that the charge transfer resistance was dominant. The high frequency plot has been associated with the charge transfer process while the low frequency loop with a slow process (mass transfer or slow homogeneous reactions). At high frequencies, the plot converged to a value on the abscissa (real axis) as shown in Fig. 7, giving the electrolytic resistance, R_Ω.

In order to determine the charge transfer resistance (R_{ct}) and the double layer capacity (C_d), we assume a Randles–Ershler type equivalent circuit, The fundamental equations including R_Ω, R_{ct} and C_d are as followings [20]:

$$\mathbf{Z}' = R_\Omega + \frac{[R_{ct} + (\sigma/\omega^{0.5})]}{\{(1 + C_d\sigma\omega^{0.5})^2 + \omega^2 C_d^2[R_{ct} + (\sigma/\omega^{0.5})]^2\}} \quad (4)$$

$$\mathbf{Z}'' = \frac{[\sigma(1 + C_d\sigma\omega^{0.5})/\omega^{0.5} + \omega C_d(R_{ct} + \sigma/\omega^{0.5})^2]}{\{(1 + C_d\sigma/\omega^{0.5})^2 + \omega^2 C_d^2[R_{ct} + (\sigma/\omega^{0.5})]^2\}} \quad (5)$$

where ω is the angular frequency, σ the constant, called the Wartburg coefficient, which is determined by the diffusion coefficients and concentrations of diffusing entities [21]. If $\omega \to \infty$, namely, the high frequency limit of the $\mathbf{Z}''$–$\mathbf{Z}'$ plot, Eqs. (4) and (5) may be simplified to give

$$\mathbf{Z}' = \frac{R_\Omega + R_{ct}}{[(\omega C_d R_{ct})^2 + 1]} \quad (6)$$

$$\mathbf{Z}'' = \frac{\omega C_d R_{ct}^2}{[(\omega C_d R_{ct})^2 + 1]} \quad (7)$$

$$\mathbf{Z}''^2 + (\mathbf{Z}' - R_\Omega - 0.5R_{ct})^2 = (0.5R_{ct})^2 \quad (8)$$

According to $dZ''/d\omega = 0$, we can find

$$C_d = \frac{1}{(\omega^* R_{ct})} \quad (9)$$

where ω^* is the angular frequency corresponding to the apex of semicircular arc.

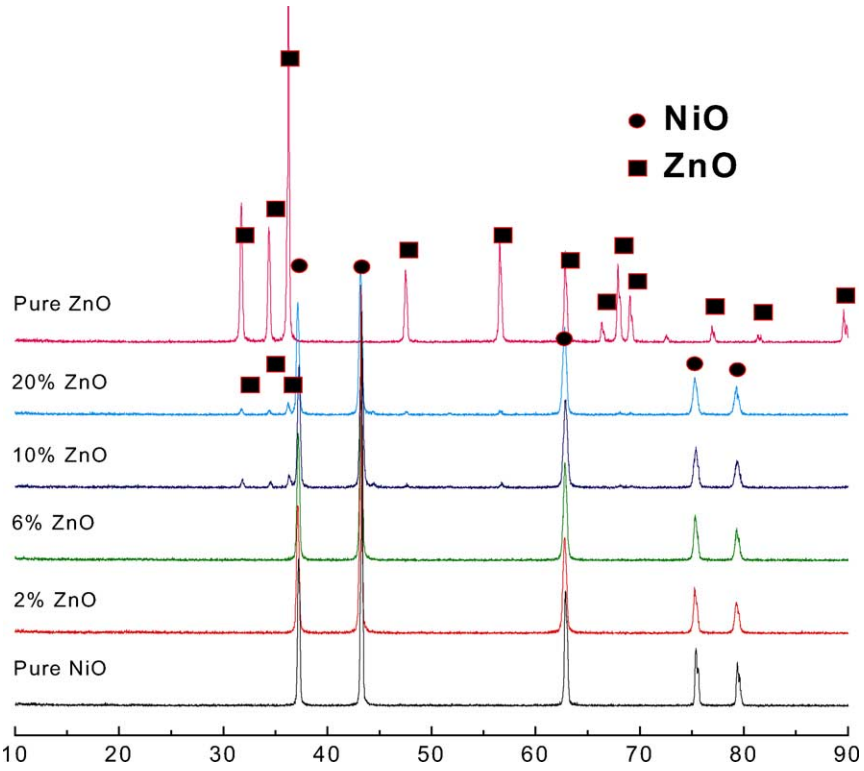

Fig. 5. XRD profiles of ZnO and ZnO/NiO cathodes before being immersed in Li/K carbonate melts.

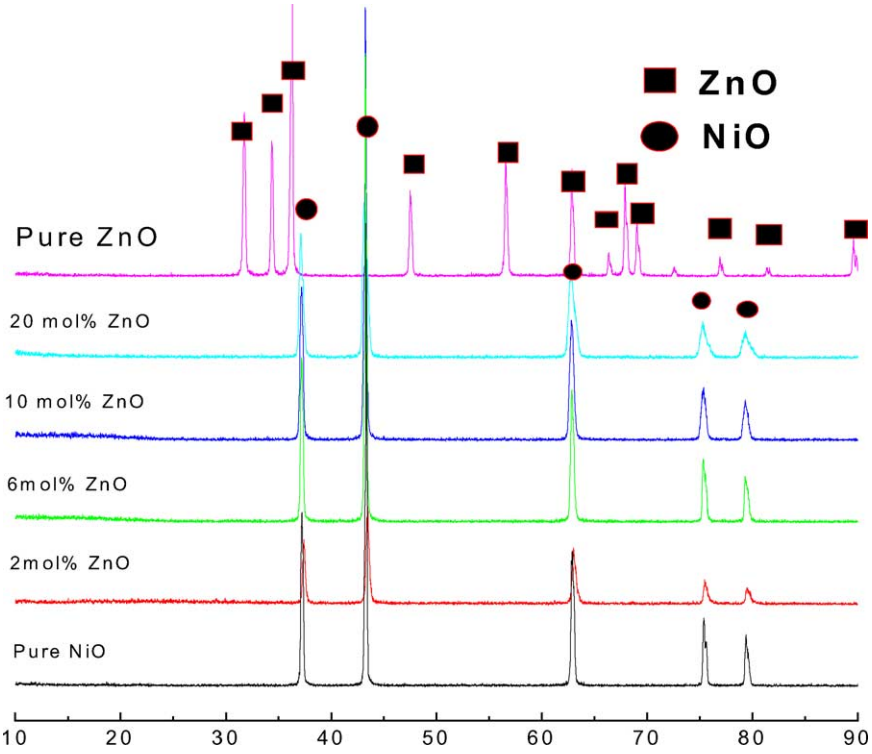

Fig. 6. XRD profiles of ZnO and ZnO/NiO cathodes immersed in Li/K carbonate melts for 200 h at 650 °C.

Using the above equation, R_Ω, R_{ct} and C_d were calculated from the high frequency limit of the $\mathbf{Z}''$–$\mathbf{Z}'$ plot. The least squares curving fitting method could be applied to obtain the optimized parameters and give the minimum deviation. Tables 3–5 summarized the fitting values of parameters for oxygen reduction on oxides electrodes in Li/K eutectic melts under a 0.67 atm CO_2/0.33 atm O_2 atmosphere at different immersion time.

According to Fig. 7 and Tables 3–5, it is apparent that the diameter of semicircular arc (denotes the charge transfer resistance R_{ct}) is decreasing sharply with time initially. This implies that, in the case of three cathode materials, the electrochemical reaction rates are increasing rapidly with time. The reason could be the incorporation of lithium in its structure, which enhances its electronic conductivity. Then, the semicircular arc increases gradually with time suggesting that the corresponding electrochemical reaction rates are decreasing slowly with time (in terms of NiO, 2 mol% ZnO/NiO, 6 mol% ZnO/NiO, after 13, 24, 50 h, respectively). The reason could be the low dissolution of nickel oxide and zinc oxide. In brief, the semicircular arc for three cathode materials shows important variations during the 100 h of immersion, which can be attributed to the changes in the structure of the reactive surface of cathode material due to the lithiation and slow dissolution of cathode material. After that, the structure seems to reach a stable state.

The influence of the ZnO content at 72 and 100 h of immersion in molten carbonate is depicted in Fig. 8. As can be seen, in the high frequency region, the semicircular arc of ZnO impregnated NiO cathode is larger than that of NiO

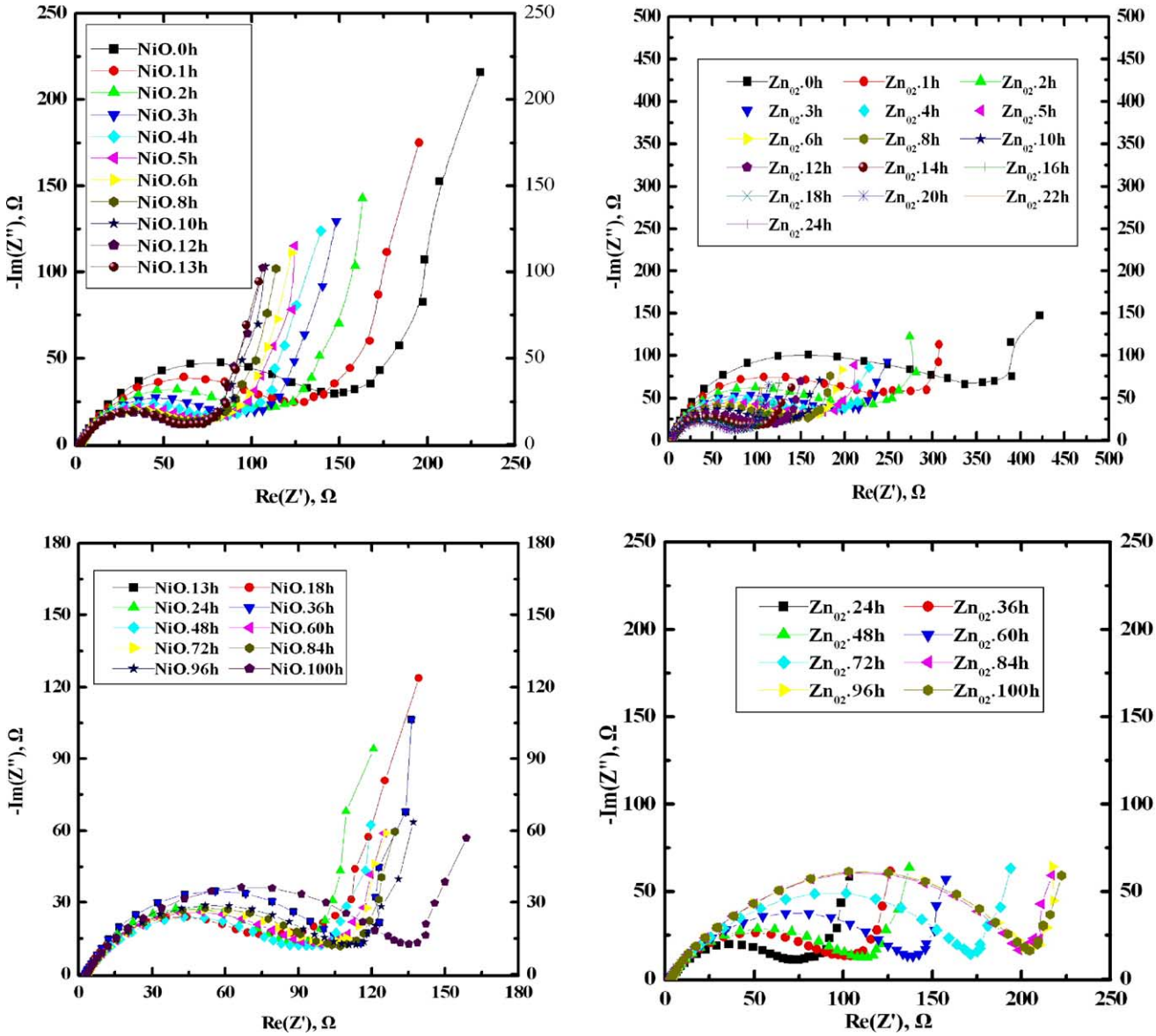

Fig. 7. Nyquist impedance spectra obtained for three samples in the frequency range of 10 mHz to 100 kHz as a function of immersion time at 650 °C in standard cathode gas atmosphere (CO_2:O_2, 67:33%). Zn_{02} denotes 2 mol% ZnO/NiO, Zn_{06} denotes 6 mol% ZnO/NiO.

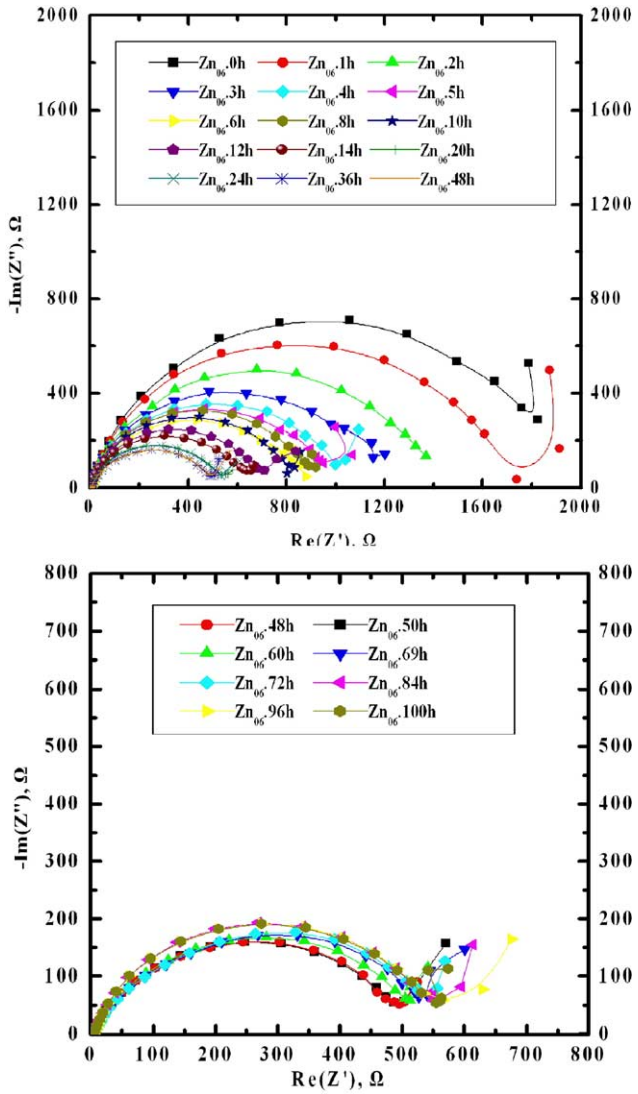

Fig. 7. (*Continued*).

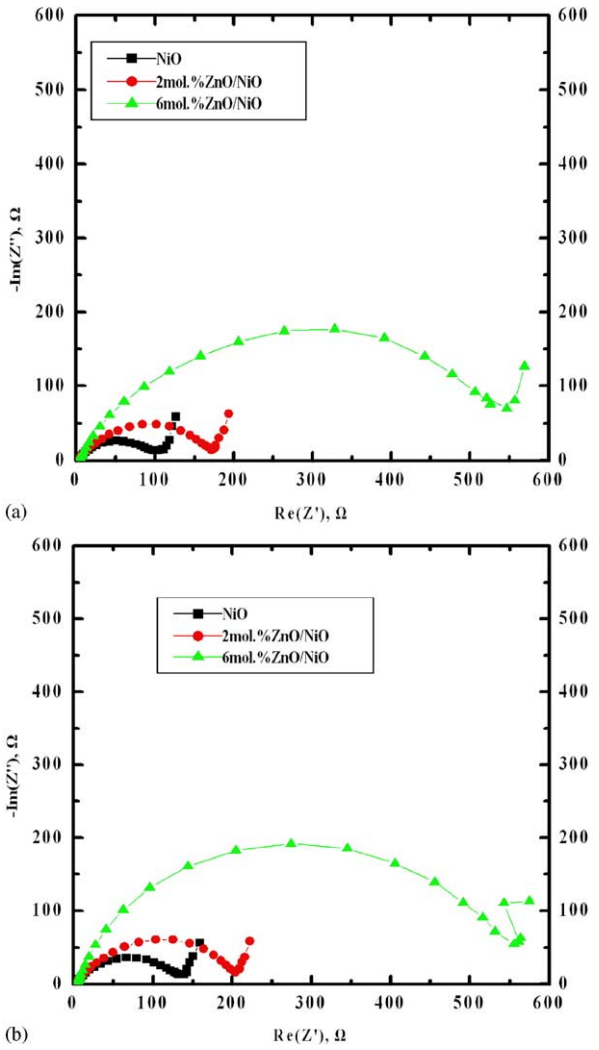

Fig. 8. Impedance spectra obtained at different immersion times: (a) 72 h;(b) 100 h.

Table 3
Fitting results for oxygen reduction on NiO electrode in Li/K eutectic melts at different immersion time (atmosphere: 0.67 atm CO_2/0.33 atm O_2; $T = 650\,^{\circ}C$)

Time (h)	$R\Omega$ (Ω)	R_{ct} (Ω)	C_d (μF)
0	2.8032	163.3	87.659
1	2.8103	128.93	83
3	2.8099	90.782	70.632
8	2.9182	63.447	63.263
13	3.0362	59.626	65.645
18	3.0213	72.557	79.609
24	3.0955	86.183	89.485
36	3.0528	107.98	88.76
48	3.1124	110.68	92.54
60	3.3215	121.35	102.44
72	3.3868	132.24	106.25
84	3.2032	135.13	114.86
96	3.1674	140.85	122.74
100	3.2867	156.87	119.89

Table 4
Fitting results for oxygen reduction on 2 mol% ZnO/NiO electrode in Li/K eutectic melts at different immersion time (atmosphere: 0.67 atm CO_2/0.33 atm O_2; $T = 650\,^{\circ}C$)

Time (h)	$R\Omega$ (Ω)	R_{ct} (Ω)	C_d (μF)
0	3.8792	275.66	110.26
2	3.7704	175.95	117.43
4	3.8731	138.98	110.34
8	3.9207	115.61	100.25
16	3.854	78.358	71.81
20	3.7288	70.382	63.481
24	3.5769	68.779	56.44
36	3.4813	91.118	55.612
48	3.2486	102.53	60.758
60	3.1259	138.03	72.383
72	3.3324	169.64	91.94
84	3.5272	201.36	117.83
96	3.5618	206.09	110.01
100	3.459	204.75	114.39

Table 5
Fitting results for oxygen reduction on 6 mol% ZnO/NiO electrode in Li/K eutectic melts at different immersion time (atmosphere: 0.67 atm CO_2/0.33 atm O_2; $T = 650\,^{\circ}C$)

Time (h)	$R\Omega$ (Ω)	R_{ct} (Ω)	C_d (μF)
0	2.1322	1906.9	108.01
2	1.7165	1397.2	112.98
4	1.6724	1029.8	107.28
8	2.3575	840.3	102.45
14	2.6223	634.6	104.23
20	2.3063	550.37	94.843
24	2.5506	537.04	96.099
36	3.1051	561.82	112.31
48	2.7733	515.46	123.31
50	3.138	511.85	126.18
60	2.9378	543.82	156.5
72	3.059	581.83	188.29
84	3.0686	584.2	188.88
96	3.136	590.24	193.39
100	3.1022	578.45	178.86

cathode. The cathode material having lower ZnO content presents smaller semicircular arc. These suggest that ZnO has a negative influence in the charge transfer processes associated with the oxygen reduction. The cathode material having 2 mol% of ZnO shows a low charge transfer resistance close to the NiO value (see Tables 3–5).

4. Conclusions

A tape casting and subsequent sintering process prepared porous nickel cathodes modified by impregnation with different content of ZnO for MCFC. The electrochemical behavior of the ex situ NiO cathodes modified by impregnation with 2–6 mol% of ZnO in the eutectic molten Li/K carbonates at 650 °C was investigated by EIS as a function of ZnO content and immersion time in the presence of standard cathode gas conditions.

The impedance spectra show modifications during the 100 h of immersion that are attributed to structural changes in the cathode surface, mainly due to the lithiation and slow dissolution of cathode material. XRD and SEM confirmed the structural and morphological changes, respectively. It has been found that the addition of ZnO to NiO considerably decreased the solubility of Ni^{2+} in the Li–K eutectic carbonate melts for the first time. The solubility of Ni^{2+} of ZnO/NiO cathode in the melt is about one order of magnitude lower than that of bare NiO cathode. The cathode material having 2 mol% of ZnO shows a very low dissolution and a small charge-transfer resistance close to the NiO value. Consequently, 2 mol% ZnO/NiO material can be regarded as an alternative material to the conventional NiO cathode in MCFCs.

Acknowledgements

This work was financially supported by the Shanghai Committee of Science and Technology and Shanghai Electric Ltd.

References

[1] Y. Ito, K. Tsuru, J. Oishi, Y. Miyazaki, K. Teruo, J. Power Sources 23 (4) (1988) 357–364.
[2] P. Ganesan, H. Colon, B. Haran, R. White, B.N. Popov, J. Power Sources 111 (2002) 109–120.
[3] A. Durairajan, H. Colon-Mercado, B. Haran, R. White, B. Popov, J. Power Sources 104 (2002) 157–168.
[4] T. Nishina, I. Uchida, Optimization of cathode gas compositions for MCFC using simplified thin film model, Denki Kagaku Oyobi Kogyo Butsuri 64 (6) (1996) 513–518.
[5] Y.H. Kim, J.R. Selman, Mechanism of low-CO_2 performance of the MCFC cathode, Proc. Electrochem. Soc. 94–13 (1994) 781–787.
[6] J.R. Selman, M.S. Alicia, Y. Lzaki, Nickel oxide cathode dissolution in the MCFC: a review, Prepr. Pap. Am. Chem. Soc., Div. Fuel Chem. 38 (4) (1993) 1429–1434.
[7] W.H.A. Peelen, M. Van Driel, K. Hemmes, J.H.W. De Wit, Electrochim. Acta 43 (21–22) (1998) 3313–3331.
[8] J.L. Smith, G.H. Kucera, A.P. Brown, in: Proceedings of the Soft-bound Series of Molten Carbonate Fuel Cell Technology, PV90-16, The Electrochemical Society, Pennington, NJ, 1990, p. 226.
[9] S. Taek Kuk, Y. Seck Song, K. Kim, J. Power Sources 83 (1999) 50–56.
[10] P. Ganesan, H. Colon, B. Haran, B.N. Popov, J. Power Sources 115 (2003) 12–18.
[11] F. Li, H.-Y. Chen, C.-M. Wang, K.-A. Hu, J. Electroanal. Chem. 531 (1) (2002) 53–60.
[12] S. Mitsushima, K. Matsuzawa, N. Kamiya, K.-I. Ota, Electrochim. Acta 47 (2002) 3823–3830.
[13] N. Motohira, T. Sensou, K. Yamauchi, K. Ogawa, X. Liu, N. Kamiya, K. Ota, J. Mol. Liq. 83 (1999) 95–103.
[14] M.J. Escudero, X.R. Nóvoa, T. Rodrigo, L. Daza, J. Power Sources 106 (2002) 196–205.
[15] L. Daza, C.M. Rangel, J. Baranda, M.T. Casais, M.J. Martínez, J.A. Alonso, J. Power Sources 86 (2000) 329–333.
[16] F. Li, C.-M. Wang, K.-A. Hu, Mater. Res. Bull. 37 (2002) 1907–1921.
[17] L. Giorgi, M. Carewska, M. Patriarca, S. Scaccia, E. Simonetti, A. Di Bartolomeo, J. Power Sources 49 (1994) 227–243.
[18] F.J. Perez, D. Duday, M.P. Hierro, J.A. Alonso, M.J. Martýnez, L. Daza, J. Power Sources 86 (2000) 309–315.
[19] A.J. Appleby, S.B. Nicholson, J. Electroanal. Chem. 53 (1974) 105.
[20] I. Uchida, T. Nishina, Y. Mugikura, K. Itaya, J. Electroanal. Chem. 206 (1986) 229–239.
[21] M. Sluyters-Rehbach, J.H. Sluyters, in: E. Yeager, J.O.'M. Bockris, B.E. Convay, S. Sarangapani (Eds.), Comprehensive Treatise of Electrochemistry, vol. 9, Plenum Press, New York, 1984, pp. 177–278.